Propionibacterium acnes Induces Autophagy in Keratinocytes: Involvement of Multiple Mechanisms

Klára Megyeri[1], László Orosz[1,7], Szilvia Bolla[2], Lilla Erdei[2], Zsolt Rázga[3], György Seprényi[4,8], Edit Urbán[5], Kornélia Szabó[6] and Lajos Kemény[2,6]

Propionibacterium acnes is a dominant member of the cutaneous microbiota. Herein, we evaluate the effects of different *P. acnes* strains and propionic acid on autophagy in keratinocytes. Our results showed that *P. acnes* strain 889 altered the architecture of the mitochondrial network; elevated the levels of light chain 3B-II, Beclin-1, and phospho-5′-adenosine-monophosphate-activated protein kinase α; stimulated autophagic flux; facilitated intracellular redistribution of light chain 3B; increased average number of autophagosomes per cell; and enhanced development of acidic vesicular organelles in the HPV-KER cell line. Propionic acid increased the level of phospho-5′-adenosine-monophosphate-activated protein kinase α, enhanced lipidation of light chain 3B, stimulated autophagic flux, and facilitated translocation of light chain 3B into autophagosomes in HPV-KER cells. *P. acnes* strains 889 and 6609 and heat-killed strain 889 also stimulated autophagosome formation in primary keratinocytes to varying degrees. These results indicate that cell wall components and secreted propionic acid metabolite of *P. acnes* evoke mitochondrial damage successively, thereby triggering 5′-adenosine-monophosphate-activated protein kinase-associated activation of autophagy, which in turn facilitates the removal of dysfunctional mitochondria and promotes survival of keratinocytes. Thus, we suggest that low-level colonization of hair follicles with noninvasive *P. acnes* strains, by triggering a local increase in autophagic activity, might exert a profound effect on several physiological processes responsible for the maintenance of skin tissue homeostasis.

Journal of Investigative Dermatology (2017) ■, ■–■; doi:10.1016/j.jid.2017.11.018

INTRODUCTION

Propionibacterium acnes is a dominant member of the cutaneous microbiota that is composed of highly variable and topographically diverse microbial communities. The skin microbiota provides colonization resistance, and thereby hampers invasion of virulent microbes. The structural components, secreted products, and metabolites of normal flora members have the potential to decrease pH; to modulate inflammation, cell viability, and differentiation; and to manipulate the virulence of pathogenic microbes. In contrast, an altered cutaneous microbiota may contribute to diseases, including acne vulgaris (Belkaid and Hand, 2014; Bouslimani et al., 2015; Christensen and Brüggemann, 2014; Oh et al., 2014; Schommer and Gallo, 2013; Szabó et al., 2017; Weyrich et al., 2015).

The skin commensal *P. acnes* is a Gram-positive, anaerobic rod that predominates in the anoxic, lipid-rich environment of sebaceous glands. *P. acnes* produces propionic acid, which protects the skin from virulent microbes. *P. acnes* carries several pathogen-associated molecular patterns, which bind to Toll-like receptor 2 (TLR2) and TLR4, leading to the production of cytokines and β-defensins (Drott et al., 2010; Kim et al., 2002; Nagy et al., 2005; Thiboutot et al., 2014). Some invasive strains interact with intracellular pathogen-associated molecular pattern sensors and trigger inflammasome assembly, stimulate a proinflammatory response, and facilitate the establishment of persistent infection (Qin et al., 2014; Tanabe et al., 2006). *P. acnes* expansion in the pilosebaceous unit can trigger tissue damage during the course of acne vulgaris (Weyrich et al., 2015). *P. acnes* has elaborated a strain-specific variability manifesting in the production of virulence determinants, cellular effects, invasiveness, and pathogenic potential. It is now widely accepted that truly commensal and pathogenic lineages of *P. acnes* exist, which can be useful members of skin microbiota and causative agents

[1]*Department of Medical Microbiology and Immunobiology, University of Szeged, Szeged, Hungary;* [2]*Department of Dermatology and Allergology, University of Szeged, Szeged, Hungary;* [3]*Department of Pathology, University of Szeged, Szeged, Hungary;* [4]*Department of Medical Biology, University of Szeged, Szeged, Hungary;* [5]*Institute of Clinical Microbiology, University of Szeged, Szeged, Hungary; and* [6]*MTA-SZTE Dermatological Research Group, Szeged, Hungary*

[7]*Current address: Public Health and Food Chain Safety Service of Government Office for Csongrád County, Laboratory Department, Derkovits fasor 7-11, Szeged, Hungary.*

[8]*Current address: Department of Anatomy, University of Szeged, Kossuth Lajos sgt. 40, Szeged, Hungary.*

Correspondence: Lajos Kemény, Department of Dermatology and Allergology, University of Szeged, Korányi fasor 6, Szeged, Hungary. E-mail: kemeny.lajos@med.u-szeged.hu

Abbreviations: AMPK, 5′-adenosine-monophosphate-activated protein kinase; BFLA, bafilomycin A1; LC3B, light chain 3B; ROS, reactive oxygen species; TLR, Toll-like receptor

Received 13 August 2017; revised 4 November 2017; accepted 6 November 2017; accepted manuscript published online 27 November 2017; corrected proof published online XXX XXXX

FLA 5.5.0 DTD ■ JID1186_proof ■ 20 December 2017 ■ 7:08 pm ■ ce

of acne vulgaris or systemic infections, respectively (Achermann et al., 2014; Beylot et al., 2014; McDowell et al., 2012).

Previous observations demonstrated that bacterial pathogen-associated molecular patterns, exotoxins, and some type 3 or type 4 secretion system effector proteins are powerful activators of autophagy. The autophagic process can function as an early antimicrobial defense pathway by targeting bacteria for autolysosomal destruction, a process known as xenophagy. Several intracellular bacteria have developed strategies with which to evade the degradative power of autophagy. These interesting studies have revealed the importance of autophagy in bacterial infections (Deretic et al., 2013; Deretic and Levine, 2009; Mathieu, 2015).

A recent study has demonstrated that a cell-invasive *P. acnes* strain triggers the accumulation of autophagosomes in Raw 264.7 macrophages, mesenchymal cells, and the HeLa cell line (Nakamura et al., 2016). Further observations have indicated that propionic acid is a powerful autophagy inducer in the HCT116 cell line. Autophagy, in response to propionic acid, was shown to develop by a succession of hierarchical steps involving mitochondrial dysfunction, reactive oxygen species (ROS) overproduction, and 5′-adenosine-monophosphate-activated protein kinase (AMPK)-mediated inhibition of the mechanistic target of rapamycin. It has also been revealed that propionic-acid-associated autophagy helps to overcome energy crisis, and promotes cell survival by blocking apoptotic demise (Tang et al., 2011). However, investigations of the pro-autophagic effects of extracellular *P. acnes* strains have not yet been reported in keratinocytes.

In this study, therefore, we investigated the effects of different *P. acnes* strains on autophagy in keratinocytes, and, in parallel, measured the involvement of the AMPK-associated autophagic pathway.

RESULTS

P. acnes induces autophagy in keratinocytes

To elucidate how live *P. acnes* strains 889 and 6609 and heat-killed strain 889 (HK-889) affect the cellular autophagic cascade, we incubated keratinocytes with bacteria in vitro at a multiplicity of infection of 100 and measured (i) the levels of microtubule-associated protein 1 light chain 3B-I (LC3B-I) and LC3B-II, (ii) autophagic flux, (iii) subcellular localization of LC3B and Beclin-1, (iv) the ultrastructural features of autophagic vacuoles, and (v) cytoplasmic acidification.

To study the effects of *P. acnes* strain 889 on basal autophagy, the levels of LC3B-I and LC3B-II were determined by western blot analysis in the HPV-KER cell line. The control cells displayed endogenous expression of both the lipidated and the nonlipidated forms of LC3B. *P. acnes*-treated cells displayed elevated LC3B-II and decreased LC3B-I levels compared with controls at each time point (Figure 1a). Furthermore, *P. acnes* strains also increased LC3B-II/LC3B-I ratios in normal human keratinocytes, live *P. acnes* strain 889 being the most powerful trigger (Supplementary Figure 1a online).

To investigate autophagic flux in cells incubated with *P. acnes* strains at 6 hpi, LC3B-II levels were measured under conditions where autophagosome degradation was blocked by bafilomycin A1 (BFLA), a pharmacological inhibitor of autophagosome-lysosome fusion and lysosomal hydrolase activity. The cultures were treated with bacteria first, and incubated with BFLA for a 4-hour period just before the preparation of cell lysates. BFLA elevated the level of LC3B-II as compared with the untreated control cells, indicating that this drug efficiently blocked autophagic flux under the experimental conditions used. In the presence of BFLA, *P. acnes* triggered a higher increase in the LC3B-II/LC3B-I ratio than that observed in the corresponding drug control (Figure 1b and Supplementary Figure 1b).

Indirect immunofluorescence assay to determine the intracellular localization of LC3B revealed that the control cells displayed a faint cytoplasmic LC3B staining; the fluorescence intensity profiles consisted of a few peaks of low height. In contrast, *P. acnes*-treated cells exhibited very bright LC3B staining; the fluorescence intensity profiles consisted of numerous robust peaks (Figure 1c, d, f, g and Supplementary Figure 2a–d online).

To investigate the effects of *P. acnes* strains on autophagosome formation, the abundances of LC3B-positive vesicles were determined. The average numbers of LC3B-positive vesicles per cell in *P. acnes*-treated cultures were significantly higher than that observed in the control cultures (Figure 1e, h and Supplementary Figure 2e, f). The live *P. acnes* strain 889 was again more efficient than strain 6609 and HK-889 in promoting the autophagic process (Supplementary Figure 2e).

Indirect immunofluorescence assay to determine the intracellular localization of Beclin-1 revealed that the control HPV-KER cells displayed a faint cytoplasmic Beclin-1 staining. In contrast, cells incubated with live *P. acnes* strain 889 exhibited very bright Beclin-1 staining; the fluorescence intensity profiles consisted of numerous robust peaks (Figure 2).

Transmission electron microscopy to investigate the ultrastructural features of autophagic compartments revealed that the control HPV-KER cells displayed a few autophagic vacuoles. In contrast, cells incubated with live *P. acnes* strain 889 exhibited a significant rise in the number of autophagosomes as early as 3 hpi and an accumulation of autolysosome stage vacuoles at 24 hpi (Figure 3). Furthermore, this test also revealed the intracytoplasmic presence of *P. acnes* partially surrounded by extensions bulging out of the endoplasmic reticulum membrane (Figure 3a). However, bacterial invasion of HPV-KER cells seems to be a rare event occurring only in the late phase of incubation.

To determine the effects of live *P. acnes* strain 889 on the formation of acidic vesicular organelles, acridine orange staining was used. In the control HPV-KER cultures, the cytoplasm stained green. In *P. acnes*-treated cells, the cytoplasm exhibited bright-red staining with a marked punctate structure (Figure 4a and b). Analysis of the fluorescence intensities in green, red, and overlapping spectral regions revealed an enhancement in red and a reduction of green fluorescence in response to *P. acnes* treatment (Figure 4c). Moreover, the average numbers of acidic vesicular organelles per cell in *P. acnes*-treated cultures were significantly higher than that observed in control cultures (Figure 4d).

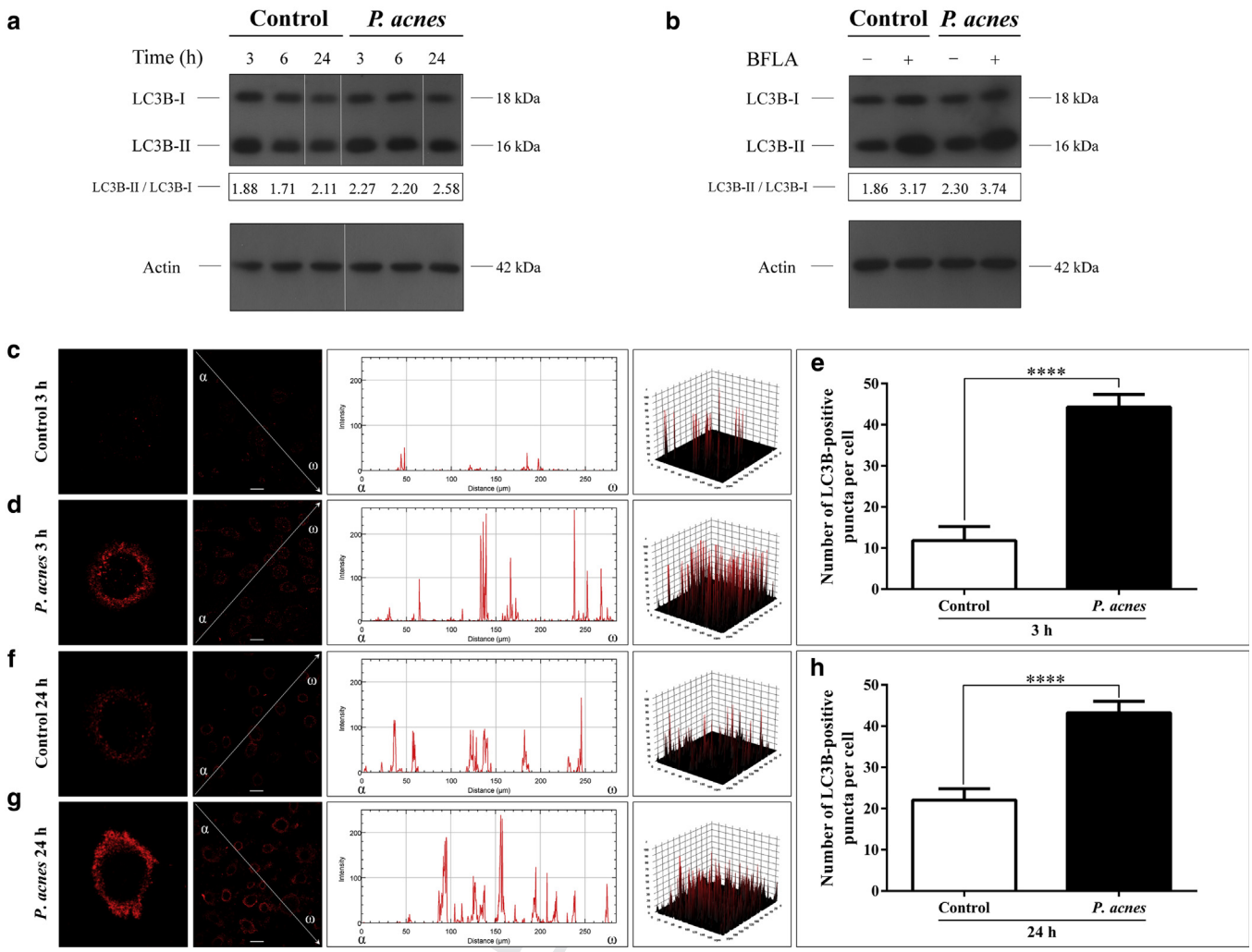

Figure 1. *P. acnes* treatment increases the LC3B-II/LC3B-I ratio, stimulates autophagic flux, and triggers autophagosome formation. (**a**) Western blot analysis showing the kinetics of LC3B-I and LC3B-II expression in control and *P. acnes*-treated cells. (**b**) Western blot analysis showing increased autophagic flux in *P. acnes*-treated cells. (**c**, **d**, **f**, **g**) Immunofluorescence assays showing the fluorescence intensities of LC3B-positive autophagic vacuoles. The line intensity scan graphs depict the intensity values along the arrows drawn across the images, whereas the 3D surface plots represent the intensity values of the whole image. (**e, h**) Immunofluorescence assays showing the average numbers of LC3B-positive autophagic vacuoles. Data are means ± standard error of the mean, n = 500. Scale bar, 10 μm. ****$P < 0.0001$. BFLA, bafilomycin A1; LC3B, light chain 3B.

P. acnes triggers abnormal mitochondrial dynamics, entailing AMPK activation and induction of autophagy

To gain some insight into the mechanism of *P. acnes*-mediated induction of autophagy, we incubated HPV-KER cells with the live strain 889 in vitro at a multiplicity of infection of 100, and measured (i) the levels of AMPKα and phospho-AMPKα (Thr172) and (ii) the ultrastructural features of mitochondria.

Western blot analysis revealed that the control cells displayed endogenous expression of both AMPKα and phospho-AMPKα (Thr172). Phosphorylation of AMPKα at Thr^{172} is known to be essential for the activation of AMPK (Stein et al., 2000). *P. acnes* triggered a pronounced increase in the level of phospho-AMPKα; the phospho-AMPKα/AMPKα ratio in *P. acnes*-treated cultures was considerably higher than that observed in controls (Figure 5a).

P. acnes induced spherical and swollen mitochondria displaying destructive changes of their cristae (Figure 5b). The median aspect ratio and form factor values in *P.* acnes-treated cultures were significantly lower than that observed in controls at the 3- and 6-hour time points (Figure 5c). To investigate further the effect of *P. acnes* on mitochondria, dot plots of aspect ratios versus form factors were generated, and divided into four quadrants defined by the 25th percentiles of the corresponding controls. The analyses of *P.* acnes-treated cells indicated a dramatic increase in the mitochondrial compartment with <25th percentile values for both aspect ratios and form factors at 3 and 6 hpi (Figure 5d). There were no significant differences in the morphological features of mitochondria between the control cells and *P. acnes*-treated cultures at 24 hpi.

Propionic acid induces autophagy in the HPV-KER cell line

To investigate the effect of propionic acid on autophagy, we treated HPV-KER cells with 10 mM propionic acid, and measured (i) the levels of LC3B-I, LC3B-II, AMPKα, and phospho-AMPKα; (ii) autophagic flux; and (iii) subcellular localization of LC3B.

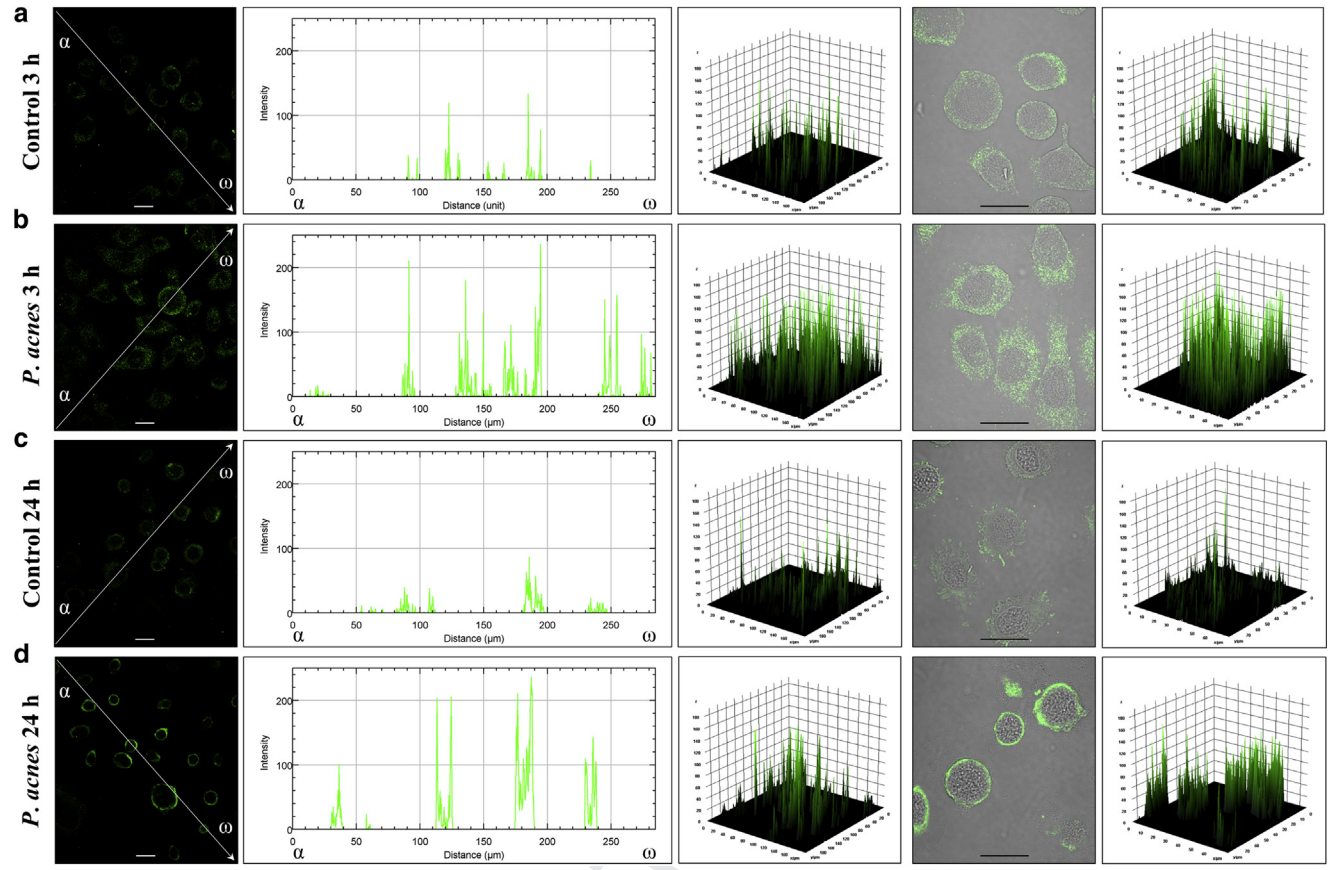

Figure 2. *P. acnes* treatment alters the intracellular distribution of Beclin-1 protein. The samples were stained for the endogenous Beclin-1 protein, and images were obtained by confocal microscopy. The images were subjected to line scan fluorescence intensity analysis and 3D surface plotting using the Image J software (Schneider et al., 2012). The line intensity scan graphs depict the intensity values along the arrows drawn across the images, whereas the 3D surface plots represent the intensity values of the whole image. Scale bar, 10 μm.

Western blot analysis revealed that propionic acid stimulated the lipidation of LC3B at the 6- and 24-hour time points, and increased autophagic flux (Figure 6a and b).

Indirect immunofluorescence assay to determine the intracellular localization of LC3B revealed that the control cells displayed a faint cytoplasmic LC3B staining at the 6-hour time point. In contrast, propionic-acid-treated cells exhibited very bright LC3B staining; the fluorescence intensity profile consisted of numerous robust peaks (Figure 6c). The average number of LC3B-positive vesicles per cell in propionic-acid-treated cultures at the 6-hour time point was significantly higher than that observed in the control cultures (Figure 6d).

To examine the involvement of AMPK in the propionic-acid-mediated induction of autophagy, the levels of AMPKα and phospho-AMPKα (Thr172) were determined by western blot analysis. Propionic acid induced moderate increases in AMPKα levels at the 3- and 6-hour time points, and triggered pronounced increases in the level of phospho-AMPKα at each time point. The phospho-AMPKα/AMPKα ratios in propionic-acid-treated cultures were considerably higher than that observed in the control cultures (Figure 6e and f).

DISCUSSION

Compelling evidence indicates that autophagy functions as an important cellular defense mechanism against the invasion of pathogenic microorganisms (Benjamin et al., 2013). Commensal bacteria were shown to exert complex effects on the autophagic activities of tissues located at the entry sites of pathogens (Benjamin et al., 2013). However, we are just beginning to understand the protective role of the pro-autophagic effect exerted by the skin microbiota. Thus, in this study, we considered the question of whether different *P. acnes* strains are able to stimulate the autophagic process in keratinocytes.

Initially, we evaluated five distinct criteria for increased autophagic activity in keratinocytes incubated with *P. acnes*. As LC3B is a well-characterized marker of autophagy (Klionsky et al., 2016), we first measured the levels of LC3B-I and LC3B-II. *P. acnes* elevated LC3B-II and decreased LC3B-I levels, indicating that the lipidation of LC3B is stimulated by live *P. acnes* strains and heat-killed bacteria. We also assessed autophagic flux in *P. acnes*-treated cultures. In the presence of BFLA, the LC3B-II level of cells incubated with *P. acnes* strains was higher than that seen in the drug control, demonstrating that autophagic flux is increased by this bacterium. Next, we performed confocal imaging to investigate the intracellular distributions of LC3B and Beclin-1. These experiments revealed that *P. acnes* raises the intensity levels of LC3B and Beclin-1 staining and stimulates translocation of these proteins into autophagosomes. Interestingly, the live *P. acnes* strain 889 was more efficient than strain 6609 and

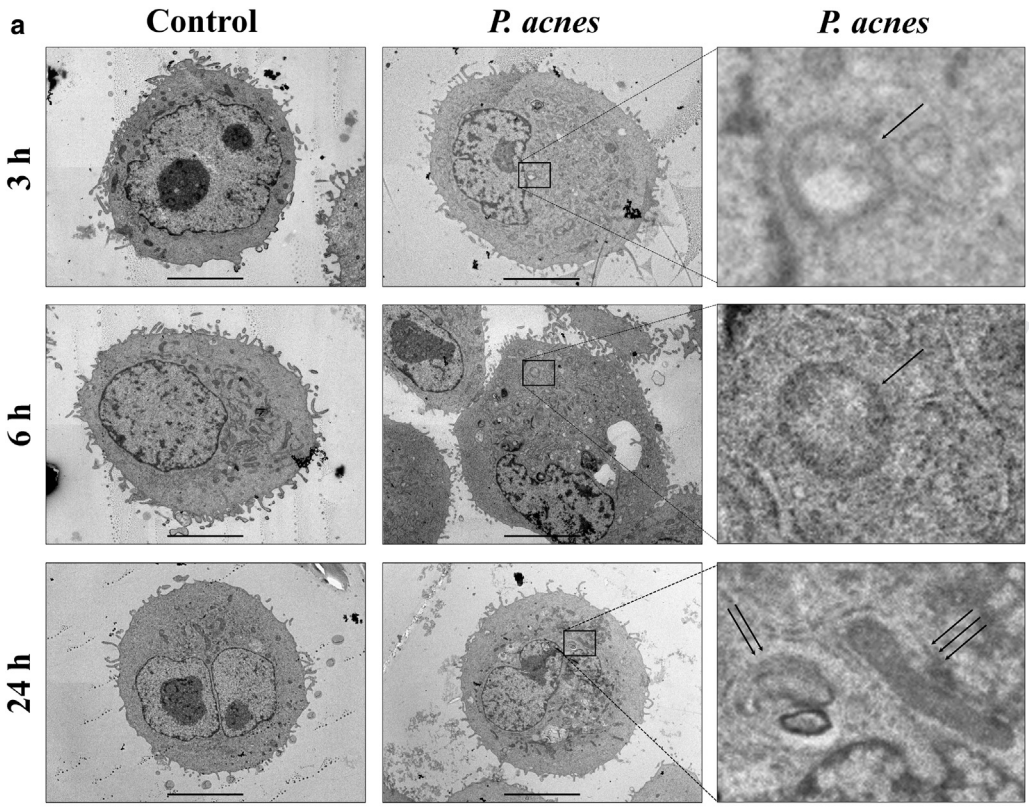

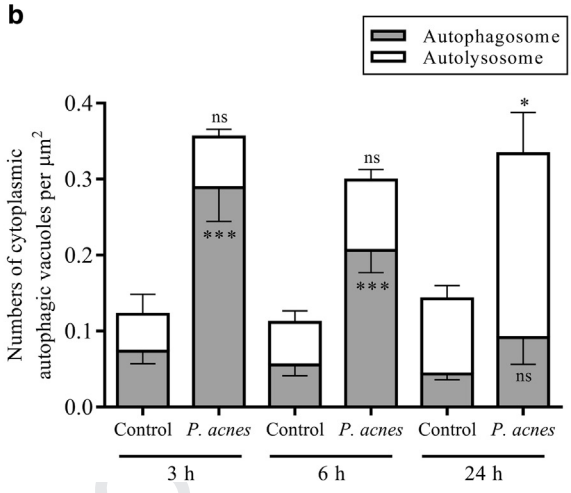

Figure 3. *P. acnes* triggers enlargement of the early and the late autophagic compartments. (**a**) Representative transmission electron microscopy micrographs depicting the ultrastructural features of autophagic compartments in control and *P. acnes*-treated cells. The solid line boxes encompassing cytoplasmic portions of cells were further enlarged in the insets to show autophagosomes, autolysosomes, and internalized bacteria denoted by single, double, and triple arrows, respectively. Scale bar, 5 µm. (**b**) Quantification of autophagic vacuoles. The total cytoplasmic areas were determined using the point-counting method, and the autophagic vacuole profiles corresponding to autophagosomes or autolysosomes were scored and counted. Data are means ± standard error of the mean, n = 10. $*P < 0.05$; $***P < 0.001$.

HK-889 in promoting autophagosome formation. In addition, we determined the effects of *P. acnes* strain 889 on acidic vesicular organelle formation. The results showed that these bacteria increase cytoplasmic acidification and enhance the development of acidic vesicular organelles. Finally, we studied the ultrastructural features of autophagic compartments by transmission electron microscopy. The data demonstrated that, at 3 and 6 hpi, *P. acnes* strain 889 triggers the accumulation of autophagosome-stage vacuoles, which subsequently evolve into degradative autolysosomes, suggesting that these bacteria trigger a transient increase in autophagic activity at the early phase of incubation, which declines thereafter. It was earlier reported that an invasive *P. acnes* strain induces autophagy in Raw 264.7 macrophages, mesenchymal cells, and HeLa cell line (Nakamura et al., 2016). Overall, our experiments demonstrate that *P. acnes* can stimulate autophagy in keratinocytes when it is present extracellularly, as the level of bacterial invasion was negligible at the low multiplicity of infection used. These results together suggest that *P. acnes*-induced autophagy might exhibit significant cell-type specificity and bacterial-strain dependency.

The diversity of bacterial structural components, secreted virulence factors, and metabolic products involved suggests a highly intricate mechanism in *P. acnes*-mediated induction of autophagy. It has already been revealed that TLR4 ligands and complex TLR2 agonists, engaging additional receptors, are strong autophagy inducers, whereas individual TLR2

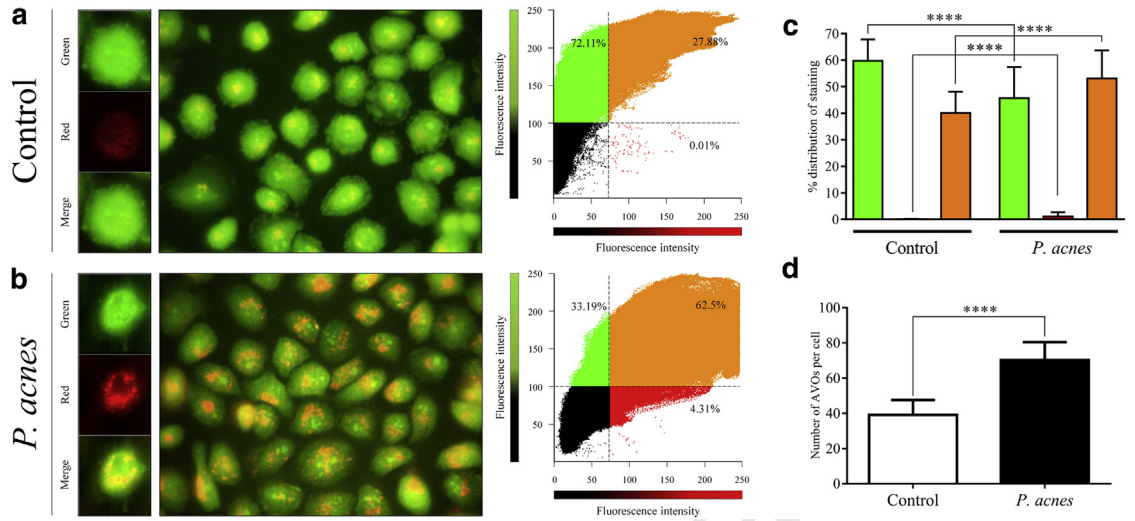

Figure 4. *Propionibacterium acnes* stimulates AVO formation. (**a**, **b**) Representative fluorescence micrographs and correlation plots showing the fluorescence intensity and intracellular localization of AVOs. Fluorescence intensities were determined and analyzed using an "apoptosis correlator" plugin (Mironova et al., 2007) operated in Image J. Thresholds indicated by dashed lines were chosen empirically so as to separate visible fluorescence from the dark pixels. (**c**) Distribution of fluorescence measured in green, red, and overlapping spectral regions. Fluorescence intensities were quantified, and the average distribution of fluorescence within the green, red, and overlapping regions was calculated. Data are means ± standard error of the mean, n = 50. (**d**) The average numbers of AVOs. Data are means ± standard error of the mean, n = 500. ****$P < 0.0001$. AVO, acidic vesicular organelle.

ligands are unable to provoke autophagy (Delgado et al., 2008). Another interesting observation clearly demonstrated that the scavenger receptor CD36 is also implicated in autophagy induction (Sanjurjo et al., 2015). CD36 functions as a TLR coreceptor and participates in the formation of the CD36-CD14-TLR2/4-TLR6 signaling module, which is capable of evoking diverse biological responses, including the increased production of ROS (Di Gioia and Zanoni, 2015). CD36 stimulates ROS generation via the nicotinamide adenine dinucleotide phosphate oxidase, whereas TLR2/4 trigger the TRAF6-ECSIT-NLRX1-dependent formation of mitochondrial ROS (Park et al., 2009; West et al., 2011). We and others have previously shown that *P. acnes* activates the TLR2/4 signal transduction mechanisms in keratinocytes (Drott et al., 2010; Kim et al., 2002; Nagy et al., 2005). Moreover, the cell wall lipoproteins of this bacterium were shown to trigger the production of ROS through the CD36 pathway (Grange et al., 2009). Excessive ROS levels might lead to mitochondrial dysfunction, which in turn evokes ATP depletion, activation of AMPK, and induction of the autophagic cascade (Inoki et al., 2003; Wang and Klionsky, 2011; Wu et al., 2014; Zhang et al., 2016; Zhao and Klionsky, 2011). It is widely accepted that AMPK-dependent autophagy functions as an important adaptive mechanism during oxidative stress by facilitating the removal of damaged mitochondria (He and Klionsky, 2009; Kroemer et al., 2010). In light of these interesting observations, we investigated how *P. acnes* affects the levels of phospho-AMPKα (Thr172) and the architecture of the mitochondrial network. Our studies have shown that the level of phospho-AMPKα (Thr172) was strongly increased in HPV-KER cells incubated with live *P. acnes* strain 889, indicating that extracellular bacteria are powerful activators of AMPK. The ultrastructural features of mitochondria were significantly altered at the early phase of *P. acnes* treatment, whereas at the late stage, the mitochondrial configurations and shape heterogeneities were largely restored. The time course of the increased autophagy level correlated well with the changes in mitochondrial morphology in *P. acnes*-treated cells. These results indicate that *P. acnes* triggers mitochondrial dysfunction and, in parallel, activates AMPK-dependent autophagy that can function as an antioxidant defense mechanism promoting the removal of damaged mitochondria.

SCFAs produced by bacterial fermentation act as signaling molecules between microbiota and host cells and regulate several specialized functions of various tissues (Ganapathy et al., 2013). The importance of commensal-derived metabolites in the regulation of autophagy is highlighted by the greatly increased autophagic activity in SCFA-treated cells (Adom and Nie, 2013; Jan et al., 2002; Tang et al., 2011). Although the level of propionic acid in the skin has not yet been determined, the propionic acid quantity in the large intestine varies between 1.5 and 26.7 mmol/kg contents (Cummings et al., 1987). Propionic acid levels can reach high concentrations at sites of bacterial colonization and infection, the subgingival concentration of this SCFA was 9.5 mM in patients with periodontal disease (Al-Lahham et al., 2010). *P. acnes* has been reported to produce 13.85 mM propionic acid during in vitro culture (Douglas and Gunter, 1946). Thus, we additionally considered the question of whether propionic acid at 10 mM concentration affects autophagy in HPV-KER cells. We found that propionic acid activated AMPK via phosphorylating AMPKα at Thr^{172}, and stimulated the lipidation of LC3B, increased autophagic flux, as well as enhanced translocation of LC3B into autophagosomes. These data demonstrate that propionic acid enhances the autophagic activity of keratinocytes via AMPK activation. Strikingly, the time course of autophagic response was different in propionic-acid- and *P. acnes*-treated keratinocytes. Thus, we suggest that this SCFA metabolite might also be implicated in the autophagic response of keratinocytes, but only after a short delay following *P. acnes* encounter.

FLA 5.5.0 DTD ■ JID1186_proof ■ 20 December 2017 ■ 7:08 pm ■ ce

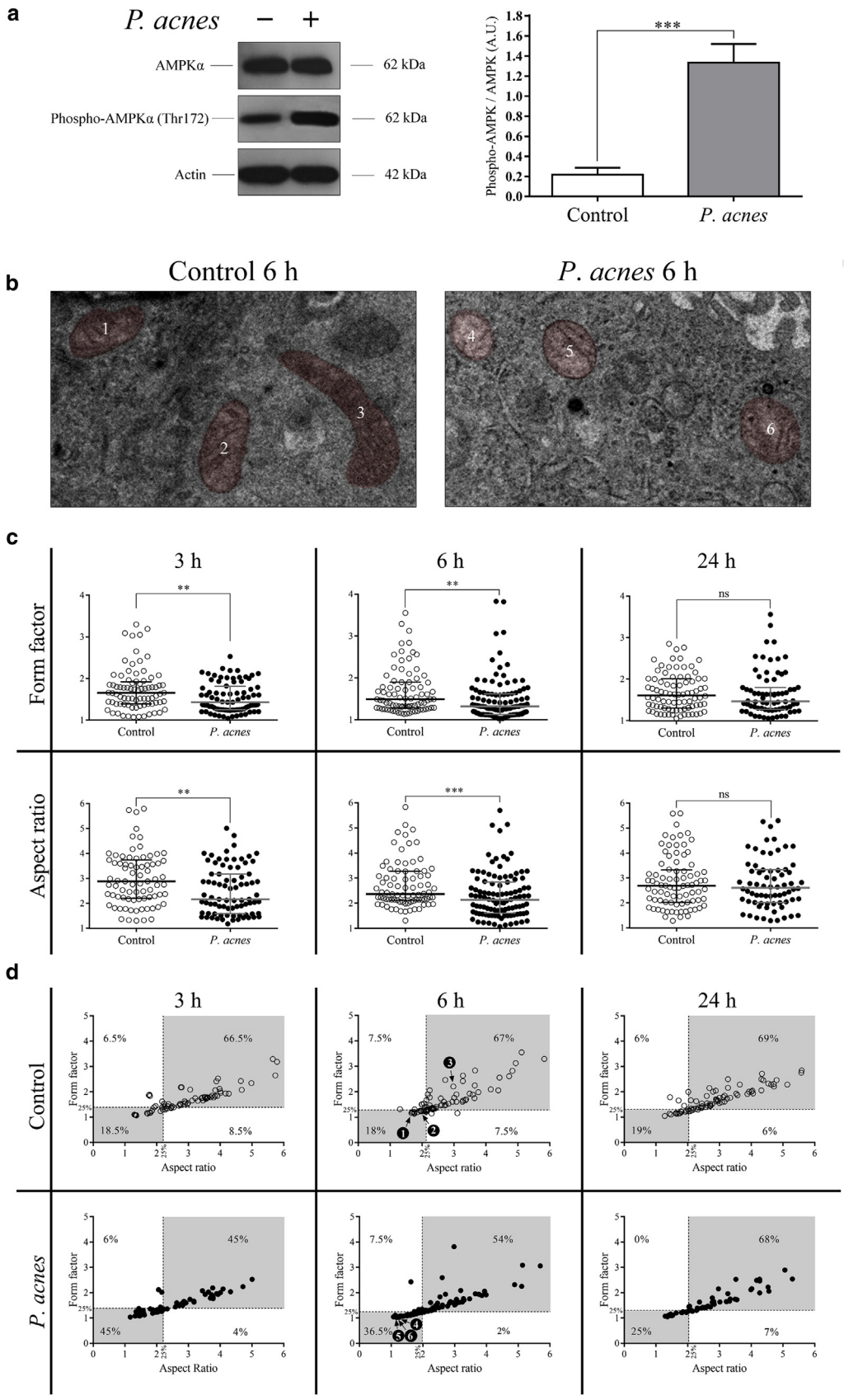

Figure 5. *Propionibacterium acnes* treatment increases the level of AMPKα phosphorylated at Thr^{172} and alters mitochondrial morphology. (**a**) Western blot analysis showing increased levels of phospho-AMPKα in *P. acnes*-treated cells. Data are means ± standard error of the mean, n = 3. (**b**) Representative transmission electron microscopy micrographs depicting the ultrastructural features of mitochondria corresponding to the numbered data points in (**d**). (**c**) Graphical representation of mitochondrial form factor and aspect ratio values. The dot plots depict the form factor and the aspect ratio values of each individual mitochondrion. The median values with interquartile ranges are shown within the graphs. (**d**) Graphical representation of mitochondrial form factor versus aspect ratio values. $^{**}P < 0.01$, $^{***}P < 0.001$. AMPK, 5′-adenosine-monophosphate-activated protein kinase; AU, arbitrary unit.

print & web 4C/FPO

FLA 5.5.0 DTD ■ JID1186_proof ■ 20 December 2017 ■ 7:08 pm ■ ce

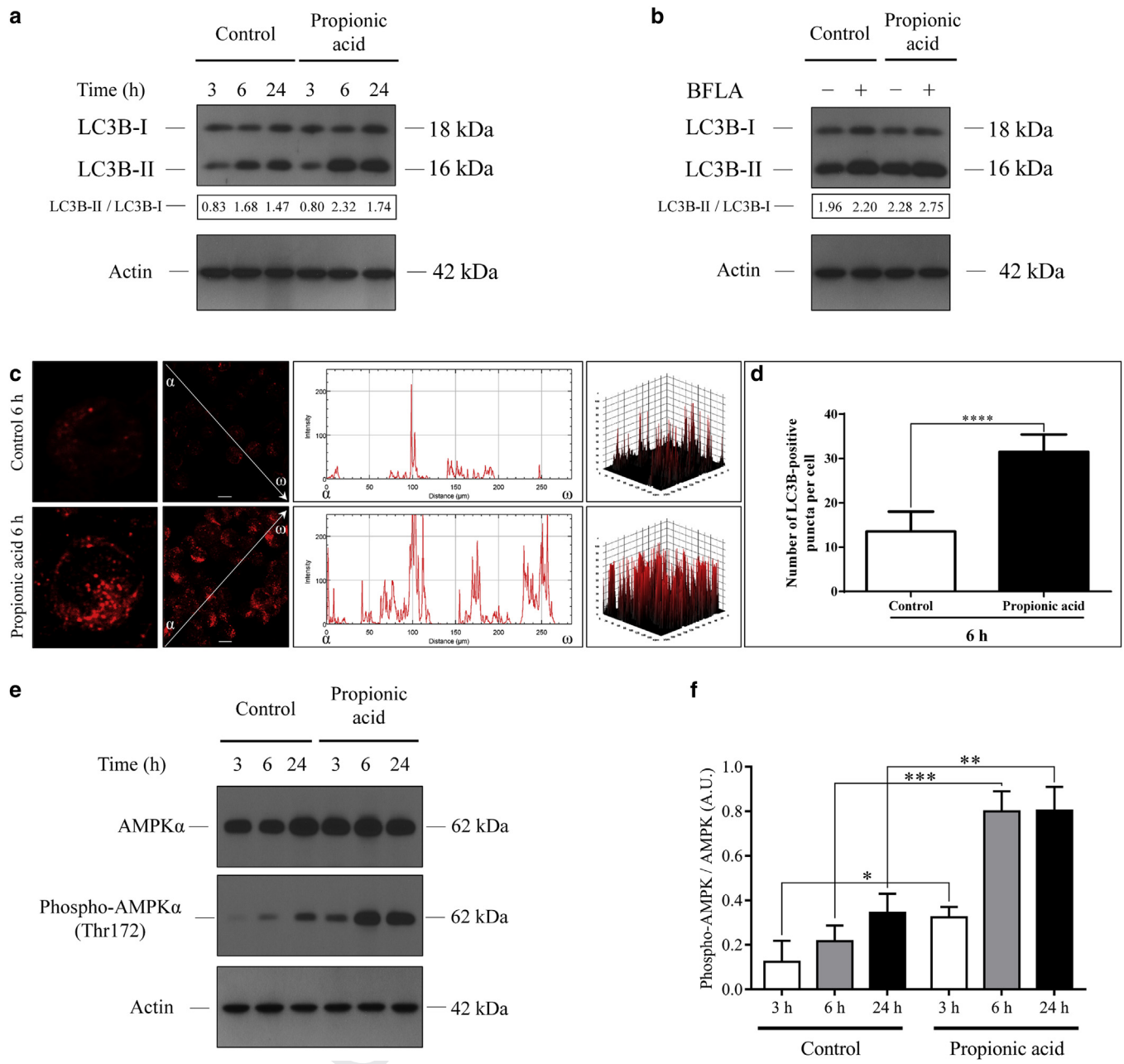

Figure 6. Propionic acid increases the LC3B-II/LC3B-I ratio, stimulates autophagic flux, and induces autophagosome formation. (**a**) Western blot analysis showing the kinetics of endogenous LC3B-I and LC3B-II expression in control and propionic-acid-treated cells. (**b**) Western blot analysis showing increased autophagic flux in propionic-acid-treated cells. (**c**) Immunofluorescence assays showing the fluorescence intensities of LC3B-positive autophagic vacuoles. (**d**) Immunofluorescence assays showing the average numbers of LC3B-positive autophagic vacuoles. Data are means ± standard error of the mean, n = 500. (**e**, **f**) Western blot analysis showing increased levels of phospho-AMPKα in propionic-acid-treated cells. Data are means ± standard error of the mean, n = 3. Scale bar, 10 μm. *$P < 0.05$; **$P < 0.01$; ***$P < 0.001$; ****$P < 0.0001$. AMPK, 5′-adenosine-monophosphate-activated protein kinase; BFLA, bafilomycin A1; LC3B, light chain 3B.

On the basis of the present results, we propose that *P. acnes* induces autophagy via its complex interactions with keratinocytes. We hypothesize that *P. acnes* stimulates the CD36-CD14-TLR2/4-TLR6 signaling module, triggers ROS generation through nicotinamide adenine dinucleotide phosphate oxidase and TRAF6-ECSIT-NLRX1 pathway, and evokes mitochondrial dysfunction. The *P. acnes*-derived propionic acid causes mitochondrial damage and aggravates oxidative stress. ROS, generated via multiple mechanisms, trigger AMPK-dependent activation of autophagy, which in turn facilitates the removal of damaged mitochondria and promotes the survival of keratinocytes (see Supplementary Figure S3 online). Thus, *P. acnes*-induced autophagy may increase the adaptive potential of keratinocytes to cope with oxidative damage.

The human skin provides an extremely potent barrier against microbial invasion because its outermost layer is composed of dead cells formed as a result of the epidermal cornification process, whereas the hair follicles can function as convenient entry sites for pathogenic bacteria (Galluzzi

FLA 5.5.0 DTD ■ JID1186_proof ■ 20 December 2017 ■ 7:08 pm ■ ce

et al., 2015; Schommer and Gallo, 2013; Szabó et al., 2017). Thus, low-level colonization of hair follicles with noninvasive *P. acnes* strains might confer remarkable antimicrobial protection by triggering a local increase in autophagic activity of keratinocytes. In addition to infectious agents, keratinocytes are also exposed to other harmful environmental stimuli, such as the UVR, chemicals, and temperature variations that lead to various pathological conditions via triggering extensive oxidative damage. Interestingly, *P. acnes* is endowed with the ability to decrease oxidative damage of bacteria and keratinocytes via the secretion of the RoxP (radical oxygenase of *P. acnes*) antioxidant enzyme (Allhorn et al., 2016). In view of the importance of autophagy in keratinocyte physiology (Li et al., 2016), the pro-autophagic effect of *P. acnes* might represent another indirect mechanism for how this commensal bacterium exerts a beneficial role in cutaneous homeostasis.

MATERIALS AND METHODS

An extended description of materials and methods is given in Supplemental Materials and Methods online.

Cell culture

The HPV-KER cell line was established and grown as previously described (Tax et al., 2016). Primary keratinocytes were obtained from healthy individuals who underwent plastic surgery after written informed consent according to the institutional review board protocol. The Medical Research Council Ethics Committee of Hungary approved the use of skin samples (ETT-TUKEB 39361). Human epidermal keratinocytes were isolated and cultured as described previously (Nagy et al., 2005). For experimental purposes, keratinocytes were cultured in antibiotic-free medium for a 24-hour period before *P. acnes* treatment.

P. acnes strain and growth conditions

P. acnes strain 889 was isolated and cultured as previously described, whereas the strain 6609 was obtained from ~~ATCC~~ (Tax et al., 2016). For experiments, keratinocytes were incubated with *P. acnes* strains at a multiplicity of infection of 100 CFU/cell. To prepare heat-killed suspensions of bacteria, *P. acnes* strain 889 was killed by incubation at 60 °C for 30 minutes.

Indirect immunofluorescence assay

Cytospin cell preparations were fixed in methanol-acetone (1:1). The slides were incubated with rabbit polyclonal antibodies to LC3B or Beclin-1 (Sigma-Aldrich, St. Louis, MO). After washing, the samples were reacted with CF640R- or CF488A-conjugated anti-rabbit antibodies (Sigma-Aldrich). The cells were visualized by confocal microscopy using an Olympus FV1000 confocal laser scanning microscope. LC3B-positive vacuoles were quantified as previously described (Orosz et al., 2016; Pásztor et al., 2014). The fluorescence intensities were determined using the line scan analysis and surface plot functions of Image J (Schneider et al., 2012).

Transmission electron microscopy

The samples were fixed, dehydrated, and embedded in Embed 812 (Electron Microscopy Sciences, Hatfield, PA). Ultrathin sections were stained with uranyl acetate and lead citrate, and examined in a JEOL JEM-1400Plus transmission electron microscope (JEOL USA, Peabody, MA). Autophagosomes and autolysosomes were scored according to their morphology. The results are presented as number of organelles/cytoplasmic area ± standard error of the mean. Mitochondrial shape descriptors were determined using Image J.

Western blot assays

Protein samples were prepared for SDS-PAGE and western blot assay as previously described (Orosz et al., 2016; Pásztor et al., 2014). The membranes were developed using a chemiluminescence detection system, the autoradiographs were scanned with a GS-800 densitometer (Bio-Rad), and band intensities were quantified using the ImageQuant software (Molecular Dynamics, Sunnyvale, CA).

Acridine orange staining

Cytoplasmic acidification was assessed by the acridine orange staining procedure as previously described (Pásztor et al., 2014). The fluorescence intensities were analyzed by using an "apoptosis correlator" plugin operated in the Image J software.

Statistical analysis

Differences in autophagic vacuole numbers and protein levels between control and *P. acnes*-treated cells were evaluated with Student's unpaired *t*-test, and the values are expressed as means ± standard error of the mean. Mitochondrial shape descriptors followed nonnormal distributions as determined by the Shapiro-Wilk normality test. Differences in aspect ratios and form factors therefore were evaluated by the Kolmogorov-Smirnov test, and the values are expressed as medians with interquartile ranges. *P*-values of less than 0.05 were considered statistically significant.

CONFLICT OF INTEREST

The authors state no conflict of interest.

ACKNOWLEDGMENTS

This work was supported by research grants OTKA 105369, GINOP-2.3.2-15-2016-00015, GINOP-2.2.1-15-2016-00007, GINOP-2.3.3-15-2016-00007, GINOP-2.3.3-15-2016-00012, and EFOP-3.6.1-16-2016-00008.

SUPPLEMENTARY MATERIAL

Supplementary material is linked to the online version of the paper at www.jidonline.org, and at https://doi.org/10.1016/j.jid.2017.11.018.

REFERENCES

Achermann Y, Goldstein EJC, Coenye T, Shirtliff ME. *Propionibacterium acnes*: from commensal to opportunistic biofilm-associated implant pathogen. Clin Microbiol Rev 2014;27:419–40.

Adom D, Nie D. Regulation of autophagy by short chain fatty acids in colon cancer cells. In: Bailly Y, editor. Autophagy—double-edged sword—cell survival or death? InTech; 2013.

Al-Lahham SH, Peppelenbosch MP, Roelofsen H, Vonk RJ, Venema K. Biological effects of propionic acid in humans; metabolism, potential applications and underlying mechanisms. Biochim Biophys Acta 2010;1801:1175–83.

Allhorn M, Arve S, Brüggemann H, Lood R. A novel enzyme with antioxidant capacity produced by the ubiquitous skin colonizer *Propionibacterium acnes*. Sci Rep 2016;6:36412.

Belkaid Y, Hand TW. Role of the microbiota in immunity and inflammation. Cell 2014;157:121–41.

Benjamin JL, Sumpter R, Levine B, Hooper LV. Intestinal epithelial autophagy is essential for host defense against invasive bacteria. Cell Host Microbe 2013;13:723–34.

Beylot C, Auffret N, Poli F, Claudel J-P, Leccia M-T, Del Giudice P, et al. *Propionibacterium acnes*: an update on its role in the pathogenesis of acne. J Eur Acad Dermatol Venereol 2014;28:271–8.

Bouslimani A, Porto C, Rath CM, Wang M, Guo Y, Gonzalez A, et al. Molecular cartography of the human skin surface in 3D. Proc Natl Acad Sci USA 2015;112:E2120–9.

Christensen GJM, Brüggemann H. Bacterial skin commensals and their role as host guardians. Benef Microbes 2014;5:201–15.

Cummings JH, Pomare EW, Branch WJ, Naylor CP, Macfarlane GT. Short chain fatty acids in human large intestine, portal, hepatic and venous blood. Gut 1987;28:1221–7.

Delgado MA, Elmaoued RA, Davis AS, Kyei G, Deretic V. Toll-like receptors control autophagy. EMBO J 2008;27:1110–21.

Deretic V, Levine B. Autophagy, immunity, and microbial adaptations. Cell Host Microbe 2009;5:527–49.

Deretic V, Saitoh T, Akira S. Autophagy in infection, inflammation and immunity. Nat Rev Immunol 2013;13:722–37.

Di Gioia M, Zanoni I. Toll-like receptor co-receptors as master regulators of the immune response. Mol Immunol 2015;63:143–52.

Douglas HC, Gunter SE. The taxonomic position of *Corynebacterium acnes*. J Bacteriol 1946;52:15–23.

Drott JB, Alexeyev O, Bergström P, Elgh F, Olsson J. *Propionibacterium acnes* infection induces upregulation of inflammatory genes and cytokine secretion in prostate epithelial cells. BMC Microbiol 2010;10:126.

Galluzzi L, Bravo-San Pedro JM, Vitale I, Aaronson SA, Abrams JM, Adam D, et al. Essential versus accessory aspects of cell death: recommendations of the NCCD 2015. Cell Death Differ 2015;22:58–73.

Ganapathy V, Thangaraju M, Prasad PD, Martin PM, Singh N. Transporters and receptors for short-chain fatty acids as the molecular link between colonic bacteria and the host. Curr Opin Pharmacol 2013;13:869–74.

Grange PA, Chéreau C, Raingeaud J, Nicco C, Weill B, Dupin N, et al. Production of superoxide anions by keratinocytes initiates *P. acnes*-induced inflammation of the skin. PLoS Pathog 2009;5:e1000527.

He C, Klionsky DJ. Regulation mechanisms and signaling pathways of autophagy. Annu Rev Genet 2009;43:67–93.

Inoki K, Zhu T, Guan K-L. TSC2 mediates cellular energy response to control cell growth and survival. Cell 2003;115:577–90.

Jan G, Belzacq AS, Haouzi D, Rouault A, Metivier D, Kroemer G, et al. Propionibacteria induce apoptosis of colorectal carcinoma cells via short-chain fatty acids acting on mitochondria. Cell Death Differ 2002;9:179.

Kim J, Ochoa M-T, Krutzik SR, Takeuchi O, Uematsu S, Legaspi AJ, et al. Activation of Toll-like receptor 2 in acne triggers inflammatory cytokine responses. J Immunol 2002;169:1535–41.

Klionsky DJ, Abdelmohsen K, Abe A, Abedin MJ, Abeliovich H, Acevedo Arozena A, et al. Guidelines for the use and interpretation of assays for monitoring autophagy (3rd edition). Autophagy 2016;12:1–222.

Kroemer G, Mariño G, Levine B. Autophagy and the integrated stress response. Mol Cell 2010;40:280–93.

Li L, Chen X, Gu H. The signaling involved in autophagy machinery in keratinocytes and therapeutic approaches for skin diseases. Oncotarget 2016;7:50682–97.

Mathieu J. Interactions between autophagy and bacterial toxins: targets for therapy? Toxins 2015;7:2918–58.

McDowell A, Barnard E, Nagy I, Gao A, Tomida S, Li H, et al. An expanded multilocus sequence typing scheme for *Propionibacterium acnes*: investigation of "pathogenic", "commensal" and antibiotic resistant strains. PLoS One 2012;7, e41480.

Mironova EV, Evstratova AA, Antonov SM. A fluorescence vital assay for the recognition and quantification of excitotoxic cell death by necrosis and apoptosis using confocal microscopy on neurons in culture. J Neurosci Methods 2007;163:1–8.

Nagy I, Pivarcsi A, Koreck A, Széll M, Urbán E, Kemény L. Distinct strains of *Propionibacterium acnes* induce selective human β-defensin-2 and interleukin-8 expression in human keratinocytes through toll-like receptors. J Invest Dermatol 2005;124:931–8.

Nakamura T, Furukawa A, Uchida K, Ogawa T, Tamura T, Sakonishi D, et al. Autophagy induced by intracellular infection of *Propionibacterium acnes*. PLoS One 2016;11:e0156298.

Oh J, Byrd AL, Deming C, Conlan S, Barnabas B, Blakesley R, et al. Biogeography and individuality shape function in the human skin metagenome. Nature 2014;514:59–64.

Orosz L, Papanicolaou EG, Seprényi G, Megyeri K. IL-17A and IL-17F induce autophagy in RAW 264.7 macrophages. Biomed Pharmacother 2016;77:129–34.

Park YM, Febbraio M, Silverstein RL. CD36 modulates migration of mouse and human macrophages in response to oxidized LDL and may contribute to macrophage trapping in the arterial intima. J Clin Invest 2009;119:136–45.

Pásztor K, Orosz L, Seprényi G, Megyeri K. Rubella virus perturbs autophagy. Med Microbiol Immunol 2014;203:323–31.

Qin M, Pirouz A, Kim M-H, Krutzik SR, Garbán HJ, Kim J. *Propionibacterium acnes* induces IL-1β secretion via the NLRP3 inflammasome in human monocytes. J Invest Dermatol 2014;134:381–8.

Sanjurjo L, Amézaga N, Aran G, Naranjo-Gómez M, Arias L, Armengol C, et al. The human CD5L/AIM-CD36 axis: a novel autophagy inducer in macrophages that modulates inflammatory responses. Autophagy 2015;11:487–502.

Schneider CA, Rasband WS, Eliceiri KW. NIH Image to ImageJ: 25 years of image analysis. Nat Methods 2012;9:671–5.

Schommer NN, Gallo RL. Structure and function of the human skin microbiome. Trends Microbiol 2013;21:660–8.

Stein SC, Woods A, Jones NA, Davison MD, Carling D. The regulation of AMP-activated protein kinase by phosphorylation. Biochem J 2000;345:437–43.

Szabó K, Erdei L, Bolla BS, Tax G, Bíró T, Kemény L. Factors shaping the composition of the cutaneous microbiota. Br J Dermatol 2017;176:344–51.

Tanabe T, Ishige I, Suzuki Y, Aita Y, Furukawa A, Ishige Y, et al. Sarcoidosis and NOD1 variation with impaired recognition of intracellular *Propionibacterium acnes*. Biochim Biophys Acta 2006;1762:794–801.

Tang Y, Chen Y, Jiang H, Nie D. Short-chain fatty acids induced autophagy serves as an adaptive strategy for retarding mitochondria-mediated apoptotic cell death. Cell Death Differ 2011;18:602–18.

Tax G, Urbán E, Palotás Z, Puskás R, Kónya Z, Bíró T, et al. Propionic acid produced by *Propionibacterium acnes* strains contributes to their pathogenicity. Acta Derm Venereol 2016;96:43–s9.

Thiboutot DM, Layton AM, Anne Eady E. IL-17: A key player in the *P. acnes* inflammatory cascade? J Invest Dermatol 2014;134:307–10.

Wang K, Klionsky DJ. Mitochondria removal by autophagy. Autophagy 2011;7:297–300.

West AP, Brodsky IE, Rahner C, Woo DK, Erdjument-Bromage H, Tempst P, et al. TLR signalling augments macrophage bactericidal activity through mitochondrial ROS. Nature 2011;472:476–80.

Weyrich LS, Dixit S, Farrer AG, Cooper AJ, Cooper AJ. The skin microbiome: associations between altered microbial communities and disease: the skin microbiome. Australas J Dermatol 2015;56:268–74.

Wu S-B, Wu Y-T, Wu T-P, Wei Y-H. Role of AMPK-mediated adaptive responses in human cells with mitochondrial dysfunction to oxidative stress. Biochim Biophys Acta 2014;1840:1331–44.

Zhang D, Wang W, Sun X, Xu D, Wang C, Zhang Q, et al. AMPK regulates autophagy by phosphorylating BECN1 at threonine 388. Autophagy 2016;12:1447–59.

Zhao M, Klionsky DJ. AMPK-dependent phosphorylation of ULK1 induces autophagy. Cell Metab 2011;13:119–20.

FLA 5.5.0 DTD ■ JID1186_proof ■ 20 December 2017 ■ 7:08 pm ■ ce